HHS Public Access

Author manuscript

*Cell Host Microbe*. Author manuscript; available in PMC 2024 April 18.

Published in final edited form as:

*Cell Host Microbe*. 2021 June 09; 29(6): 930–940.e4. doi:10.1016/j.chom.2021.03.007.

# Interaction between *Staphylococcus* Agr virulence and neutrophils regulates pathogen expansion and skin inflammation

**Masanori Matsumoto**[1,*], **Seitaro Nakagawa**[1], **Lingzhi Zhang**[1], **Yuumi Nakamura**[2], **Amer E. Villaruz**[3], **Michael Otto**[3], **Christiane Wolz**[4], **Naohiro Inohara**[1], **Gabriel Núnez**[1,*,‡]

[1]Department of Pathology and Rogel Cancer Center, The University of Michigan Medical School, Ann Arbor, MI 48109, USA

[2]Cutaneous Immunology, Immunology Frontier Research Center, Osaka University, Osaka, 565-0871, Japan

[3]Pathogen Molecular Genetics Section, Laboratory of Human Bacterial Pathogenesis, National Institute of Allergy and Infectious Diseases, National Institutes of Health, Bethesda, MD 20892, USA.

[4]Interfakultäres Institut für Mikrobiologie und Infektionsmedizin, Tübingen, Germany

## Summary

The skin is a common site of infection by *Staphylococcus aureus*, but the host-pathogen interactions that control pathogen growth and invasion remain poorly understood. We found a differential requirement for quorum-sensing Agr virulence and specifically PSMα peptides for pathogen growth and induction of inflammation in the skin. In neutrophil-deficient mice, *S. aureus* growth on the epidermis was unaffected, but the pathogen penetrated into the dermis and subcutaneous tissue which required PSMα. In the dermis, pathogen expansion required Agr virulence in wild-type, but not neutrophil-deficient mice. Mechanistically, Agr virulence limited oxidative and non-oxidative killing in neutrophils by inhibiting pathogen late endosome localization and promoting phagosome escape into the cytosol. Unlike Agr, SaeR/S virulence was not required for pathogen growth in the epidermis, and promoted dermal pathogen growth independently of neutrophils. Thus, *S. aureus* growth and invasion are regulated distinctly by different virulence systems in the skin. Agr limits intracellular pathogen killing in neutrophils to promote pathogen expansion in the dermis and subcutaneous tissue.

[*]Corresponding author: masanori@umich.edu (M.M), gabriel.nunez@umich.edu (G.N.).
[‡]Lead author

Author Contributions

Designed experiments, M.M. and G.N.; Performed experiments, M.M. and L.Z.; Provided critical reagents and scientific insight, Y.N., A.V., M.O. and C.W.; Analyzed data, M.M., S.N., N.I. and G.N.; M.M. and G.N. wrote the paper.

Competing Financial Interests

The authors declare no competing financial interests.

**Keywords**

Agr virulence; neutrophils; phenol-soluble modulins; SaeR/S virulence; *Staphylococcus aureus* ; skin infection; skin inflammation

## Introduction

*Staphylococcus aureus,* a Gram-positive bacterium, is a major human pathogen causing significant morbidity and mortality in both community and hospital-acquired infections (Lowy, 1998). The skin is a major infection site for *S. aureus* that can colonize the epidermis of about 10% of healthy individuals (Lowy, 1998). *S. aureus* can produce several virulence factors which can help the pathogen to breach the epidermal barrier and invade the dermis and deeper tissues thereby causing a wide range of systemic infections (Balasubramanian et al., 2017). One major *S. aureus* virulence program is the quorum-sensing (QS) accessory gene regulatory (Agr) system that is activated in response to bacterial density (Novick, 2003). Upon stimulation by the auto-inducing peptide (AIP), the receptor kinase AgrC activates the response regulator AgrA to induce the expression of the *agrBDCA* operon that induces virulence factors via the regulatory RNAIII (Boisset et al., 2007). In addition, AgrA activates the promoters of genes encoding phenol-soluble modulins (PSMs), a group of amphipathic α-helical peptides that include PSMα, PSMβ and δ-toxin (Queck et al., 2008). The four PSMα1-4 peptides are highly cytotoxic to a wide variety of cells including keratinocytes and phagocytes (Nakagawa et al., 2017; Nakamura et al., 2013; Wang et al., 2007). In the epidermis, Agr-regulated PSMα induces keratinocyte damage leading to the release of the alarmins IL-36 and IL-1α that triggers skin inflammation (Liu et al., 2017; Nakagawa et al., 2017). Agr is involved in the development of *S. aureus* infection in several tissues (Abdelnour et al., 1993; Gillaspy et al., 1995; Heyer et al., 2002) and Agr and PSMs are particularly crucial for the development of subcutaneous infection, epidermal *S. aureus* colonization and induction of skin inflammation (Cheung et al., 2011; Kobayashi et al., 2011; Li et al., 2016; Nakagawa et al., 2017; Nakamura et al., 2020; Wang et al., 2007). However, the host immune mechanisms that limit pathogen invasion into the dermis remain unclear. Furthermore, the pathogen-host interactions that regulate *S. aureus* expansion in the dermis remain poorly understood.

Neutrophils play a critical role in the initial phase of host defense against bacterial pathogens. The importance of neutrophils in limiting *S. aureus* infection is highlighted by the observation that patients with neutropenia or genetic defects that impair pathogen killing are highly susceptible to infections (Curnutte et al., 1974; Hill et al., 1974; Howard et al., 1977; Introne et al., 1999). Upon infection with *S. aureus*, neutrophils are rapidly recruited to the site of infection where they engulf and kill the internalized pathogen via several mechanisms. These include the production of reactive oxygen species (ROS) through the assembly of the phagocyte nicotinamide adenine dinucleotide phosphate ($NADP^+$) oxidase complex, and the delivery of a plethora of bactericidal molecules inside the phagosome (Ley et al., 2018). To counter these immune protective mechanisms, *S. aureus* has evolved multiple and often redundant strategies to evade pathogen killing inside the phagosome including production of molecules that counter ROS and modifications of the cell wall that

increase the resistance of the pathogen to antimicrobial molecules (Beavers and Skaar, 2016; Foster et al., 2014). Phagosomal escape is another strategy by which *S. aureus* can limit intracellular killing (Horn et al., 2018). Several pathogen factors have been suggested to play a critical role in inducing the translocation of *S. aureus* from the phagosome to the cytosol (Horn et al., 2018). Of these factors, Agr-induced PSMα peptides have been identified as critical mediators of *S. aureus* phagosomal escape in both epithelial cells and phagocytes *in vitro* (Blattner et al., 2016; Grosz et al., 2014; Munzenmayer et al., 2016; Surewaard et al., 2013). However, the host cells targeted by Agr virulence to promote pathogen growth in vivo remain unclear. In the current work, we show specific interaction of Agr virulence with neutrophils regulates pathogen expansion and inflammation in the skin. Furthermore, we show a different function of Agr virulence in the epidermis and the dermis during *S. aureus* infection.

## Results

### Differential role of neutrophils in epidermal and intradermal *S. aureus* infection.

To assess the role of neutrophils in epidermal infection, we compared the epicutaneous and intradermal models of *S. aureus* colonization using *S. aureus* (strain LAC, pulsed-field type USA300). In the intradermal model, $10^6$ colony-forming units (cfu) of *S. aureus* were inoculated into the dermis and lesion size, neutrophil infiltration and pathogen loads were assessed overtime after infection. We observed a peak in lesion size, skin inflammation and neutrophil infiltration on day 2 which correlated with pathogen loads (Figures 1A-1D). In the epicutaneous model, $10^6$ cfu of *S. aureus* are applied to the surface of the epidermis with a gauze to enhance colonization, but without physical disruption of the epidermis using a protocol that induces Agr virulence (Nakamura et al., 2013). In this gauze-supported skin colonization model, we found that disease score, pathogen loads and neutrophil infiltration increased overtime when assessed on day 0, 2, 4 and 7 after epidermal colonization (Figures 1E-1H). To examine the role of neutrophils, WT mice were treated with anti-Ly6G monoclonal antibody (Mab) to deplete neutrophils or isotype-matched control Mab. Administration of anti-Ly6G Mab depleted ~80% of $CD11b^+Gr1^+$ neutrophils in the skin of infected mice when compared with mice treated with control antibody (Figure S1A). As expected, depletion of neutrophils was associated with an increase in the size of the skin lesions after intradermal inoculation which correlated with increased pathogen loads (Figures 1I-1K). In contrast, we found that in the epicutaneous colonization model, depletion of neutrophils was associated with reduced skin inflammation and disease scores, but similar pathogen loads when compared with that observed in mice treated with control antibody (Figures 1L-1N).

We next assessed the localization of *S. aureus* after epicutaneous and intradermal inoculation using immunohistochemical analysis. As expected, the bacterium was detected in the dermis in close association with neutrophils after intradermal infection (Figure S1B). In contrast, *S. aureus* localized to the epidermal surface after epicutaneous colonization (Figure S1B). We reasoned that antibiotics will be unable to kill *S. aureus* in the epicutaneous model given its superficial localization. Intraperitoneal administration of vancomycin abrogated *S aureus* colonization and pathogen-induced inflammation in the intradermal model (Figures

S1C-S1E), but had no effect in either disease score or *S. aureus* loads in the epicutaneous model (Figures S1F-S1H). The nicotinamide adenine dinucleotide phosphate (NADPH) oxidase is critical for phagosomal bacteria killing via oxidative burst in neutrophils (Soehnlein and Lindbom, 2010). Deficiency in Cybb/Nox2, an essential component of the multi-unit NADPH oxidase complex, impaired *S. aureus* clearance and enhanced lesion size after intradermal inoculation (Figures S1I-S1L). In contrast, $Cybb^{-/-}$ mice and WT mice exhibited comparable pathogen loads and disease scores after epicutaneous inoculation (Figures S1M-S1P). These results indicate that neutrophils play a differential role in the epicutaneous and intradermal *S. aureus* colonization models.

## Neutrophils are required to prevent *S. aureus* invasion into the dermis.

Administration of anti-Ly6G Mab induces ~ 80% depletion of neutrophils (Figure S1A). We hypothesized that residual neutrophils in mice treated with anti-Ly6G Mab may be sufficient to control pathogen infection in the presence of the epidermal barrier. To test this hypothesis, we generated mice lacking neutrophils by deleting Mcl1, an antiapoptotic Bcl-2 member that is required for neutrophil survival (Dzhagalov et al., 2007). To generate neutrophil-deficient mice, we crossed *Mcl1* floxed mice ($Mcl1^{f/f}$) with $Mrp8^{Cre/+}$ mice that drive Cre expression specifically in neutrophils (Csepregi et al., 2018). Flow cytometric analysis revealed that $CD11b^{+}Ly6G^{+}$ neutrophils were absent in the bone marrow, blood and spleen of $Mrp8^{Cre/+}Mcl1^{f/f}$ mice (Figures S2A and S2B). Furthermore, epicutaneous inoculation with *S. aureus* induced robust recruitment of neutrophils in the skin of $Mcl1^{f/f}$ mice, but minimal or no neutrophil infiltration was observed in $Mrp8^{Cre/+}Mcl1^{f/f}$ mice while the numbers of monocytes and macrophages in the skin were comparable in both groups of mice (Figure S2C). Neutrophil-deficient $Mrp8^{Cre/+}Mcl1^{f/f}$ mice inoculated intradermally with *S. aureus* developed large ulcerated skin lesions associated with abundant numbers of bacteria below the epidermis and a marked increase in pathogen loads when compared with neutrophil-sufficient $Mcl1^{f/f}$ mice (Figures 2A-2C). While *S. aureus* was only detected on the surface of the epidermis in $Mcl1^{f/f}$ mice after epicutaneous inoculation, $Mrp8^{Cre/+}Mcl1^{f/f}$ mice showed marked invasion of *S. aureus* into the dermis and underlying soft tissue (Figure 2D and S2D). Although the skin lesions were smaller in $Mrp8^{Cre/+}Mcl1^{f/f}$ mice than in $Mcl1^{f/f}$ mice, they contained numerous erosions in the epidermis (Figure 2E). The total pathogen loads in the skin tissue were comparable in $Mrp8^{Cre/+}Mcl1^{f/f}$ and $Mcl1^{f/f}$ mice (Figure 2F). Consistent with local penetration of *S. aureus* into the dermis and underlying soft tissue, we detected higher pathogen numbers in the spleen, kidney and liver of $Mrp8^{Cre/+}Mcl1^{f/f}$ mice than in $Mcl1^{f/f}$ mice after epicutaneous colonization (Figure S2D). We also compared in the same experiments the phenotype of $Mrp8^{Cre/+}Mcl1^{f/f}$ neutrophil-deficient and $Cybb^{-/-}$ mice after *S. aureus* dermal inoculation. Both mutant mice showed larger skin lesion and increased pathogen loads compared to WT mice, but neutrophil-deficient mice exhibited larger lesions with more pathogen loads than $Cybb^{-/-}$ mice (Figures S2E-S2G). These results indicate that neutrophils are required to prevent invasion of *S. aureus* into the dermis and systemic tissues after epidermal colonization. Furthermore, the studies suggest that neutrophils control pathogen growth through oxidative and non-oxidative killing in the dermis.

## Agr-regulated PSMα peptides are required for pathogen dermal invasion in the absence of neutrophils.

The QS Agr system regulates the production of a wide array of virulence factors including PSMs that are important for pathogen growth in animal tissues (Novick, 2003; Le et al. 2015) We next asked whether Agr virulence is required for *S. aureus* invasion into the dermis and soft tissue in the absence of neutrophils. In these experiments, we inoculated *Mcl1*$^{f/f}$ and *Mrp8*$^{Cre/+}$*Mcl1*$^{f/f}$ mice epicutaneously with WT or isogenic *S. aureus* strains deficient in Agr virulence or the production of Agr-regulated PSMα or PSMβ peptides. In neutrophil-sufficient mice, the *agr* and *psm*α deficient strains, but not the *psm*β mutant strain were impaired in inducing inflammatory skin disease which correlated with reduced *S. aureus* colonization after epicutaneous inoculation (Figures 3A-3C). While the WT bacterium and the *psm*β mutant invaded the dermis and underlying soft tissue in *Mrp8*$^{Cre/+}$*Mcl1*$^{f/f}$ neutrophil-deficient mice, the *agr* and *psm*α deficient strains did not (Figures 3D-3F). These results indicate that Agr virulence and specifically PSMα peptides are required for *S. aureus* invasion into the dermis and soft tissue in neutrophil-deficient mice colonized epicutaneously with the pathogen.

## Agr virulence is not required for intradermal *S. aureus* growth in the absence of neutrophils.

We next assessed the role of Agr virulence in intradermal *S. aureus* infection in the presence or absence of neutrophils. We inoculated *Mcl1*$^{f/f}$ and *Mrp8*$^{Cre/+}$*Mcl1*$^{f/f}$ mice intradermally with WT and isogenic *S. aureus agr* mutant strains and assessed the ability of bacteria to colonize the skin and underlying soft tissue and induce skin disease. In neutrophil-sufficient *Mcl1*$^{f/f}$ mice, the *agr* and *psm*α deficient strains, but not the *psm*β mutant were impaired in inducing skin disease which correlated with a marked reduction in pathogen colonization (Figures 4A-4C). In contrast, the *agr* and *psm*α deficient strains colonized the dermis and subcutaneous soft tissue and elicited skin lesions to levels that were comparable to those observed with the WT bacterium in neutrophil-deficient *Mrp8*$^{Cre+}$*Mcl1*$^{f/f}$ mice (Figures 4D-4F and S3). These results indicate that Agr virulence is required for *S. aureus* growth and skin pathology after intradermal inoculation in the presence, but not in the absence of neutrophils.

## Contrasting roles of Agr and SaeR/S virulence in pathogen colonization and skin inflammation.

*S. aureus* also uses the SaeR/S regulatory system to produce a variety of virulence factors that are important for immune evasion and pathogen growth in host tissues (Guerra et al., 2017). SaeR/S does not impact on *psm* expression, but is required for expression of many toxins and immune modulatory proteins import for pathogen growth (Munzenmayer et al., 2016). We next assessed the ability of SaeR/S virulence to promote *S. aureus* skin colonization in the presence and absence of neutrophils. In WT mice, the *saeR/S* mutant strain elicited reduced skin disease after epidermal colonization, but pathogen colonization was comparable to that observed with the WT bacterium (Figures 5A-5C). The reduced inflammation observed with the *saeR/S* mutant correlated with impaired recruitment of neutrophils to the skin (Figure S4A). In contrast to the *agr* mutant, the *S. aureus* strain

lacking saeR/S virulence retained its ability to invade into the dermis and soft tissue after epidermal colonization in neutrophil-deficient *Mrp8*$^{Cre/+}$*Mcl1*$^{f/f}$ mice (Figures 5A-5C). In the intradermal model, the *saeR/S*-deficient strain was impaired in eliciting skin disease and neutrophil infiltration which was associated with markedly reduced pathogen colonization in WT mice (Figures 5D-5F and Figure S4B). In contrast to the *agr* mutant, the *saeR/S*-deficient strain was greatly impaired in inducing skin disease after intradermal inoculation in *Mrp8*$^{Cre/+}$*Mcl1*$^{f/f}$ neutrophil-deficient mice (Figures 5D-5F). Furthermore, unlike the *agr* mutant, the ability of the *S. aureus saeR/S* mutant to colonize the dermis and subcutaneous tissue was also reduced impaired in *Mrp8*$^{Cre/+}$*Mcl1*$^{f/f}$ mice (Figures 5D-5F). These results indicate that SaeR/S virulence is not required for dermal invasion after epicutaneous inoculation in the absence of neutrophils. Furthermore, SaeR/S-regulated virulence is critical for intradermal pathogen growth and skin disease both in the presence and absence of neutrophils.

## Agr virulence limits neutrophil phagosomal killing in neutrophils.

The finding that Agr virulence is not required for pathogen growth in the absence of neutrophils suggested that a main function of Agr is to evade pathogen killing by neutrophils. Quantitative RT-PCR analysis revealed that expression of *psmα* was increased in a time-dependent manner in neutrophils after *S. aureus* infection (Figure 6A). This is in contrast to *saeR* and s*aeS* expressions that declined in neutrophils after infection (Figure 6A). The expression of Agr virulence in vitro was consistent with the observation that *psmα* was detected in vivo after intradermal inoculation of a *psmα*-lux *S. aureus* reporter strain in WT mice, but much less in neutrophil-deficient mice (Figure 6B). The reduced expression of *psmα* in neutrophil-deficient mice was verified in dermal tissue using quantitative RT-PCR analysis (Figure 6C). These results suggest that expression of *S. aureus* PSMα is positively regulated in neutrophils in vivo. To assess the function of Agr virulence in neutrophils, we incubated primary mouse neutrophils with WT and *agr* mutant *S. aureus* strains at a moi of 5 for 15 min, removed extracellular bacteria by extensive washing and assessed the number of intracellular and extracellular bacteria after pathogen uptake. We found that the uptake of the WT and mutant *S. aureus* strains by neutrophils was comparable when assessed 20 min after incubation (Figure S5A). In contrast, the numbers of intracellular and extracellular *agr* and *psmα* mutant, but not *psmβ*-deficient, bacteria were reduced compared to the WT bacterium when assessed 80 min after infection (Figure 6D). In contrast, the numbers of intracellular and extracellular *seaR/S* mutant bacteria were comparable to those observed with the WT bacterium when assessed 80 min after incubation with neutrophils (Figure S5B). To determine whether Agr virulence regulates the localization of *S. aureus* inside neutrophils, we incubated primary neutrophil preparations with yellow fluorescence protein (YFP)-labeled WT and *agr* mutant strains and assessed their intracellular localization by fluorescence microscopy. Because the neutrophil preparations contain ~ 80% neutrophils, we incubated the cells with APC-labeled anti-Ly6G antibody to identify neutrophils in these preparations. At 20 min post incubation, the number of bacteria inside neutrophils and the percentage of neutrophils in which the intracellular pathogen co-localized with LAMP-1, a marker of late-endosomes and lysosomes, were comparable in neutrophils incubated with the WT and the *agr* mutant strains (Figure S5C). Likewise, the numbers of WT and *agr* mutant strain co-localizing with Rab5, a marker of early endosomes was comparable 20

min after incubation (Figure S5D). After 80 min incubation, the percentage of neutrophils containing high number (greater than 10) bacteria of the WT strain was higher than of the *agr* mutant strain (Figure 6E). Conversely, the percentage of neutrophils harboring low number (5 or less) of the *agr* mutant strain was higher than that of the WT strain (Figure 6E). Notably, the percentage of neutrophils in which the pathogen co-localized with LAMP-1 was higher in the *agr* mutant than in the WT without an increase in neutrophil cytotoxicity (Figure 6E, right panel, and S5E). These results suggest that Agr virulence limits the localization of *S. aureus* in late endosome promoting phagosome escape into the cytosol and extracellular space.

## Agr virulence limits oxidative and non-oxidative killing in vivo.

A main mechanism of pathogen killing inside the neutrophil phagosome is mediated via NADPH oxidase-dependent oxidative burst (Ley et al. 2018). To assess the role of Agr virulence in the regulation of oxidative killing, we infected WT and neutrophils deficient in Cybb/Nox2, an essential molecule of the NAPDH oxidase complex with WT and *agr* mutant *S. aureus* strains. We found that the uptake of the WT and *agr* mutant *S. aureus* strains by WT and $Cybb^{-/-}$ neutrophils was comparable when assessed 20 min after incubation (Figure S6A). After 80 min incubation, however, the numbers of intracellular and extracellular WT and *agr* mutant *S. aureus* were higher in $Cybb^{-/-}$ neutrophils than in WT neutrophils (Figure 7A). Notably, the numbers of intracellular and extracellular *agr* mutant bacteria in $Cybb^{-/-}$ neutrophils were comparable or higher than of the WT bacteria in WT neutrophils (Figure 7A). Cytotoxicity of $Cybb^{-/-}$ neutrophils treated with WT and *agr* mutant *S. aureus* was higher than that observed in WT neutrophils (Figure S6B). We next assessed the number and localization of WT and *agr* mutant S. *aureus* in WT and $Cybb^{-/-}$ neutrophils by fluorescence microscopy. After 80 min incubation, the percentage of neutrophils containing greater than 10 bacteria of the WT strain was higher than of the *agr* mutant strain in both WT and $Cybb^{-/-}$ neutrophils (Figure 7B). Conversely, the percentage of neutrophils harboring low number of bacteria (5 or less) of the WT strain was lower than of the *agr* mutant strain in both WT and $Cybb^{-/-}$ neutrophils (Figure 7B). Notably, the percentage of neutrophils harboring high number (more than 10) of *agr* mutant *S. aureus* in $Cybb^{-/-}$ neutrophils was comparable to that of the WT bacterium in WT neutrophils (Figure 7B). Furthermore, the percentage of neutrophils in which bacteria co-localized with LAMP-1 was higher in the *agr* mutant than in the WT bacterium in both WT and $Cybb^{-/-}$ neutrophils (Figure 7B, right lower panel).

We showed in Figure 4 that Agr virulence is not required for growth of *S. aureus* in the dermis in the absence of neutrophils suggesting that this virulence programs targets killing by neutrophils. Therefore, we assessed whether Agr virulence limits pathogen killing via the phagosomal NAPDH oxidase complex in vivo. In these experiments, we inoculated WT and $Cybb^{-/-}$ mice with WT and *agr* mutant *S. aureus* intradermically and assessed skin disease and pathogen loads. In accord with results shown in Figures S1I-S1K, the disease scores and pathogen loads observed after inoculation with the WT bacterium were higher in $Cybb^{-/-}$ mice than in WT animals (Figures 7C-7E). In accord with results shown in Figures 4A-4C, the *agr* mutant bacterium was impaired in triggering skin disease which was associated with markedly reduced pathogen loads in WT mice (Figures 7C-7E). Importantly, the loads of the *agr* mutant strain were ~ 100-fold higher in $Cybb^{-/-}$ mice than in WT mice which was

associated with higher lesion sizes (Figure 7E). However, the loads and lesion sizes with the *agr* mutant strain in *Cybb*$^{-/-}$ mice were almost comparable to those observed with the WT bacterium in WT mice (Figures 7D and 7E). Together the results suggest that Agr virulence limits both oxidative and non-oxidative killing in neutrophils to expand in the dermis.

## Discussion

Although most *S. aureus* infections originate in the skin, the pathogen-host interactions that regulate pathogen invasion from the skin surface to the dermis and underlying tissues remain poorly understood. In the current work, we show that neutrophils play a critical role in preventing the invasion of the pathogen from the epidermis to the dermis. Although QS Agr virulence was required for pathogen invasion into the dermis and for pathogen expansion in both the epidermis and the dermis, we found a differential requirement for Agr virulence in the absence of neutrophils. In the epidermis, Agr-regulated cytopathic PSMα peptides were required for pathogen growth independently of the presence of neutrophils while in the dermis Agr virulence was dispensable for pathogen expansion in the absence of neutrophils. Cytopathic PSMα peptides are important for keratinocyte damage and the subsequent release of keratinocyte alarmins to induce inflammation after epidermal colonization (Nakagawa et al., 2017). Because the surface of the epidermis is scarce in nutrients, the requirement of Agr-regulated PSMα peptides suggests that these cytopathic peptides also induce the release of nutrients or other factors from keratinocytes to sustain robust growth of *S. aureus* on the epidermal surface. The host molecules that enable pathogen growth in the epidermis remain to be determined.

Earlier studies showed that PSMα peptides induce robust killing of a variety of immune and non-immune cells *in vitro* (Nakagawa et al., 2017; Nakamura et al., 2013; Wang et al., 2007), suggesting that Agr virulence is used by the pathogen to target host cells. However, the relevance of these findings for the regulation of pathogen growth in vivo remained unclear. The lack of requirement of Agr virulence for pathogen growth and induction of skin disease after dermal inoculation in the absence of neutrophils suggests that a main function of Agr virulence in vivo is to evade killing of the pathogen by neutrophils. Our studies are consistent with previous work that identified Agr-induced PSMα peptides as critical mediators of *S. aureus* phagosomal escape in phagocytic cells in vitro (Blattner et al., 2016; Grosz et al., 2014; Surewaard et al., 2013), although these previous studies did not assess the relevance of these findings *in vivo*. We further show that the presence of Agr virulence reduced the co-localization of *S. aureus* with LAMP1, a marker of late endosomes, in neutrophils. Collectively, these observations suggest that membrane-rupturing PSMα peptides induced via Agr virulence limit the degradation of the pathogen in late endosomes and lysosomes by promoting its escape from the phagosome to the cytosol. We found an increased in extracellular bacteria after infection of neutrophils with WT *S. aureus* compared with *agr* mutant bacteria, suggesting that Agr virulence also promotes the release of *S. aureus* from the cytosol to the extracellular compartment. The release of WT *S. aureus* into the extracellular space mediated by Agr is likely to promote pathogen spread *in vivo*. Previous work with human neutrophils showed marked lysis of the cells after *S. aureus* infection with CA-MRSA strain MW2 which was largely dependent on Agr virulence (Surewaard et al., 2013). We did not observe increased cytotoxicity of mouse

neutrophils incubated with WT *S. aureus* compared with the *agr* mutant bacterium under our *in vitro* conditions. The reason for the difference in results is not clear, but it could be explained by host species, pathogen strain or subtle differences in the experimental conditions. Analyses of neutrophils and mice deficient in the NAPDH oxidase complex that kills bacteria via oxidative burst in the phagosome revealed that Agr virulence limits the killing of *S. aureus* via both oxidative and non-oxidative mechanisms in neutrophils. Although the non-oxidative killing mechanisms are regulated by Agr virulence, neutrophils can kill bacteria through several processes including activation of myeloperoxidase, delivery of anti-microbial molecules into the phagosome and the release of neutrophil extracellular traps (Ley et al., 2018). Further studies are needed to understand the individual contribution of the non-oxidative processes and whether Agr virulence can subvert such mechanisms to promote pathogen growth *in vivo*.

Our studies revealed a contrasting role of Agr and SaeR/S virulence in the regulation of pathogen growth and inflammatory disease in the skin (Figure S6C). While Agr virulence was required for pathogen growth in WT mice and dermal invasion in neutrophil-deficient mice, SaeR/S was dispensable for both activities after epidermal colonization. Furthermore, although both virulence programs were required for dermal pathogen expansion in WT mice, the SaeR/S system was necessary for dermal expansion and skin disease in the absence of neutrophils while Agr virulence was not. These results suggest that a main function of Agr virulence in the dermis and subcutaneous tissue is to promote pathogen growth by subverting pathogen killing mechanisms in neutrophils while SaeR/S virulence may act by targeting different cells or processes in the host. In the absence of neutrophils and Agr virulence, these observations suggest that SaeR/S drives pathogen expansion in the dermis as this virulence program was required for *S. aureus* growth after dermal inoculation. The contrasting role of Agr and SaeR/S virulence in skin infection may be explained by differences in the expression and function of these virulence programs in host cells during infection. Consistent with previous studies (Surewaard et al., 2012), we found that *psmα* is induced after phagocytosis in neutrophils *in vitro*. In addition, we observed reduced expression of *psmα* in the skin of neutrophil-deficient mice supporting the notion that Agr virulence is induced in neutrophils *in vivo*. Inside host cells and presumably neutrophils the concentration of the quorum sensing pheromone AIP can reach the critical concentration necessary for *agr* activation (Carnes et al., 2010; Pang et al., 2010). Furthermore, *S. aureus* produces (p)ppGpp as a messenger of environmental stress conditions which appears important for the induction of PSMs in the neutrophil phagosome (Geiger et al., 2012). While Agr-induced PSMα peptides form α-helical structures that disrupt hydrophobic membranes without host cell specificity (Peschel and Otto, 2013), the cytolytic activity of SaeR/S-regulated pore-forming toxins including Panton-Valentine leucocidin (PVL) and the leukocidins LukSF and LukAB recognize specific receptors on host cells and display a more restricted species and host cell specificity (Cho et al., 2015; Geiger et al., 2012; Nygaard et al., 2010). For example, a major role of SaeR/S-regulated LukAB and PVL in the escape of *S. aureus* from human macrophages (Munzenmayer et al., 2016). Thus, SaeR/S-regulated virulence may act to subvert pathogen killing in macrophages or other host cells. However, further studies are needed to determine the mechanism by which SaeR/S virulence limits pathogen killing in vivo.

In conclusion, we show that a distinct role of Agr virulence in the colonization of the epidermis and dermis and a key role of neutrophils in preventing invasion of *S. aureus* into the dermis. Notably, Agr virulence was not required for pathogen expansion in the dermis in the absence of neutrophils suggesting that this virulence program targets neutrophils to limit pathogen killing via oxidative and non-oxidative killing. The function of Agr virulence is in contrast to that of the saeR/S system that is not required for epidermal colonization or pathogen invasion into the dermis and promotes pathogen expansion independently of neutrophils. Further studies are needed to understand the mechanism by which Agr promotes pathogen growth in the epidermis and limits non-oxidative killing by neutrophils.

## STAR METHODS

### CONTACT FOR REAGENT AND RESOURCING SHARING

Further information and requests for resources and reagents should be directed to and will be fulfilled by the Lead Contact, Gabriel Nunez (gabriel.nunez@umich.edu).

### EXPERIMENTAL MODELS AND SUBJECTS DETAILS

**Animals—**C57BL/6 mice were purchased from the Jackson Laboratory and expanded in our mouse facility at the University of Michigan. *Cybb*$^{-/-}$ mice were purchased from the Jackson Laboratory. *Mrp8*$^{Cre/+}$*Mcl1*$^{f/f}$ mice on C57BL/6 background were kindly provided by Dr. Andres Hidalgo, Centro Nacional de Investigaciones Cardiovasculares (CNIC), Madrid. All mice were maintained under specific pathogen-free conditions and were used at 8 to 12 weeks of age. All animal studies were performed according to approved protocols by the University of Michigan Review Board for Animal Care.

### METHOD DETAILS

**Antibody treatment—**For antibody-mediated depletion, antibodies were purchased from BioXCell. To deplete neutrophils, mice were treated with anti-Ly6G antibody (250 μg) (clone: 1A8) intraperitoneally on day −1, 1, 3 and 5 before and after *S. aureus* infection.

**Cell isolation and flow cytometric analysis—**For isolation of skin mononuclear cells, skin tissues were digested with 1.0 Wunsch units/ml Liberase DH (Roche) and 100 μg/ml DNase I (Sigma) at 37°C for 1h. The cells were resuspended on a Percoll gradient (75%/40%) (GE Healthcare) and centrifuged at 2000 rpm for 20 min at 25°C. Single-cell suspensions from skin, blood, bone marrow and spleen were stained with the following fluorochrome-conjugated antibodies purchased from BD Biosciences, Biolegend, or eBioscience: Allophycocyanin (APC)-conjugated anti-Ly6G (1A8) and anti-Ly6C (AL-21); Fixable Viability Dye eFluor 780; fluorescein isothiocyanate (FITC)-conjugated anti-CD11b (M1/70); Peridinin chlorophyll protein complex-cyanin 5.5 (PerCP5.5)-conjugated anti-CD4 (RM4-5); phycoerythrin (PE)-conjugated anti-B220 (RA3-6B2), anti-F4/80 (BM8) and anti-Gr1 (RB6-8C5); PE-Cy7-conjugated anti-CD8 (53-6.7); violet 450-conjugated anti-Ly6G (1A8). The cells were then analyzed on a LSRII flow cytometer (BD Biosciences).

**Immunohistochemical analysis—**Frozen skin sections were fixed with acetone, labeled with polyclonal biotin-conjugated anti-*S. aureus* antibody (Abcam) at 4°C overnight and

then stained with FITC-conjugated streptavidin (Invitrogen). In some experiments, skin sections were stained with PE-conjugated anti-Ly6G antibody (1A8). For nuclear staining, DAPI (Invitrogen) was used. Images of stained sections were viewed with a fluorescence microscope BZ-X700 (Keyence).

***S. aureus* colonization—**The methicillin-resistant *Staphylococcus aureus* strain USA300 (LAC), the isogenic *agr*, *psma*, *psmβ* and *saeR/S* mutant strains and YFP-WT and YFP-*agr* mutant strains have been described (Nygaard et al., 2010; Wang et al., 2007). For epicutaneous colonization, bacteria were grown for 4 hrs in tryptic soy broth with shaking at 37°C. Mice were colonized on the shaved dorsal skin of mice by applying a 1 $cm^2$ sterile gauze containing 1 x $10^6$ cfu of *S. aureus* which was covered with occlusive plastic dressing (Tegaderm; 3M). In some experiments, mice were intradermally injected with 1 x $10^6$ efu of *S. aureus*. For treatment with vancomycin, vancomycin (100 mg/kg) was injected intraperitoneally 30 min before *S. aureus* inoculation. To determine bacterial numbers in the colonized skin, spleen, kidney and liver, the tissues were collected from individual mice, homogenized in cold PBS and plated at serial dilution onto Mannitol-salt agar containing 10% egg yolk. The number of cfu was determined after 48 h of incubation at 37°C. Mice were sacrificed on day 7 day after colonization, and skins were assessed in a blinded fashion using a scoring system described previously (Nakamura et al., 2013). Briefly, 4 points were used to denote the severity of erythema (0, none; 1, mild; 2, moderate; 3, severe), scaling (0, none; 1, mild; 2, moderate; 3, severe), erosion (0, none; 1, mild; 2, moderate; 3, severe), edema (0, none; 1, mild; 2, moderate; 3, severe), and thickness (0, none; 1, mild; 2, moderate; 3, severe). Skin samples were fixed in 10% formalin and processed for HE and Gram staining or frozen sections were obtained for immunohistochemistry.

**Quantitative real-time PCR with reverse transcription—***S. aureus* strains were grown overnight in tryptic soy broth with shaking at 37°C. In some experiments, neutrophils cultured with the serum-treated *S. aureus* were treated with recombinant TNF-α (Biolegend; 1 μg/ml) for the indicated time, washed with RPMI medium 2 times and then lysed with 0.1% TritonX-100 in PBS prior to isolation of *S. aureus* RNA. RNA isolation of *S. aureus* treated with lysozyme (15 mg/ml) and lysostaphin (1 mg/ml) for 30 min at 37°C was performed with E.Z.N.A. Bacterial RNA kit according to the manufacturer's instructions (OMEGA). The complementary DNA was synthesized using a High Capacity RNA-to-cDNA Kit (Applied Biosystems) according to the manufacturer's instructions. Quantitative real time (RT)-PCR was performed using a TaqMan PCR master mix (Applied Biosystems) and StepOne Real-time PCR system (Applied Biosystems). Primers to amplify bacterial genes (*psmα*, *saeR*, *saeS* and *gyrB*) have been described (Dastgheyb et al., 2015; Nygaard et al., 2010). *psmα*, *saeR* and *saeS* expression was normalized to that of *S. aureus gyrB* and relative expression calculated by the 2-ΔΔCt method.

***S. aureus* killing assay—**WT LAC and its isogenic mutant strains ($10^9$ cfu/ml) were incubated with equal amount of serum from WT mice for 15 min. Neutrophils (5 x $10^6$) enriched from the bone marrow of WT mice by Neutrophil Isolation Kit (Miltenyi Biotec) were cultured with serum-treated *S. aureus* at a moi of 5 for 15 min, washed with RPMI medium and then treated with recombinant TNF-α (1 μg/ml) for 1 h. After

centrifugation, the supernatant and neutrophils were diluted with 0.1% TritonX-100 in PBS and the numbers of extracellular bacteria in supernatant and intracellular bacteria in neutrophils were assessed by serial plating on MSA plates. In some experiments, neutrophils cultured with YFP-A *aureus* were stained with APC-conjugated anti-Ly6G antibody, fixed with 4% paraformaldehyde, treated with 0.1% saponin, incubated with rabbit anti-Rab5 antibody, stained with DAPI and Alexa Fluor 555-conjugated anti-rabbit IgG or PE-labeled anti-LAMP-1 antibody, and viewed with confocal microscope A1 (Nikon).

**Cytotoxicity Assay—**Cytotoxicity was measured by a lactate dehydrogenase (LDH) cytotoxicity detection kit (Takara Biochemicals). Neutrophils were cultured with *S. aureus* and LDH release assay was performed according to the manufacturer's instructions.

**Measurement of *psmα*-lux expression—**For in vivo bioluminescence imaging, mice were intradermally inoculated with 1 x $10^6$ LAC *psmα*-lux strain (Dastgheyb et al., 2015), killed on day 2 after infection, and immediately placed into the light-tight chamber of the CCD (charge-coupled device) camera system (IVIS200, PerkinElmer). Luminescence emitted from lux-expressing bacteria in the tissue was quantified using the software program Living Image (PerkinElmer).

**Quantification and statistical analyses—**Statistical analyses were performed using GraphPad Prism software version 5.0 (GraphPad Software Inc.). Differences between two groups were evaluated using Student's t test (parametric) or Mann-Whitney U test (non-parametric). For multiple comparisons, statistical analysis was performed using one-way ANOVA (parametric) or Kruscal-Wallis test (non-parametric), and then Bonferroni test for parametric samples, or Dunn's test for non-parametric samples as a post-hoc test. Differences at $P<0.05$ were considered significant.

## Supplementary Material

Refer to Web version on PubMed Central for supplementary material.

## Acknowledgments

The authors thank the University of Michigan Flow Cytometry Core for Flow cytometry analysis. This work was supported by JSPS KAKENHI; Grant Number 26713038 (Y.N.), 16H06252 (Y.N.), AMED-PRIME JP18gm6010016h0002 (Y.N.), the Naito Foundation (Y.N.), the Uehara Memorial Foundation (M.M.), Mochida Memorial Foundation for Medical and Pharmaceutical Research (M.M.) and NIH grant AR069303 (G.N.). Y.N. and S.N. were supported by the Institute for Global Prominent Research, Chiba University. S.N. was supported by the Leading Graduate School Program of Chiba University (Nurture of Creative Research Leaders in Immune System Regulation and Innovative Therapeutics). M.O. was supported by the Intramural Research Program of the National Institute of Allergy and Infectious Diseases, US National Institutes of Health (grant number ZIA AI000904-16).

## References

Abdelnour A, Arvidson S, Bremell T, Ryden C, and Tarkowski A (1993). The accessory gene regulator (agr) controls Staphylococcus aureus virulence in a murine arthritis model. Infect Immun 61, 3879–3885. [PubMed: 8359909]

Balasubramanian D, Harper L, Shopsin B, and Torres VJ (2017). Staphylococcus aureus pathogenesis in diverse host environments. Pathog Dis 75.

Beavers WN, and Skaar EP (2016). Neutrophil-generated oxidative stress and protein damage in Staphylococcus aureus. Pathog Dis 74.

Blattner S, Das S, Paprotka K, Eilers U, Krischke M, Kretschmer D, Remmele CW, Dittrich M, Muller T, Schuelein-Voelk C, et al. (2016). Staphylococcus aureus Exploits a Non-ribosomal Cyclic Dipeptide to Modulate Survival within Epithelial Cells and Phagocytes. PLoS Pathog 12, e1005857. [PubMed: 27632173]

Boisset S, Geissmann T, Huntzinger E, Fechter P, Bendridi N, Possedko M, Chevalier C, Helfer AC, Benito Y, Jacquier A, et al. (2007). Staphylococcus aureus RNAIII coordinately represses the synthesis of virulence factors and the transcription regulator Rot by an antisense mechanism. Genes Dev 21, 1353–1366. [PubMed: 17545468]

Carnes EC, Lopez DM, Donegan NP, Cheung A, Gresham H, Timmins GS, and Brinker CJ (2010). Confinement-induced quorum sensing of individual Staphylococcus aureus bacteria. Nat Chem Biol 6, 41–45. [PubMed: 19935660]

Cheung GY, Wang R, Khan BA, Sturdevant DE, and Otto M (2011). Role of the accessory gene regulator agr in community-associated methicillin-resistant Staphylococcus aureus pathogenesis. Infect Immun 79, 1927–1935. [PubMed: 21402769]

Cho H, Jeong DW, Liu Q, Yeo WS, Vogl T, Skaar EP, Chazin WJ, and Bae T (2015). Calprotectin Increases the Activity of the SaeRS Two Component System and Murine Mortality during Staphylococcus aureus Infections. PLoS Pathog 11, e1005026. [PubMed: 26147796]

Csepregi JZ, Orosz A, Zajta E, Kasa O, Nemeth T, Simon E, Fodor S, Csonka K, Baratki BL, Kovesdi D, et al. (2018). Myeloid-Specific Deletion of Mcl-1 Yields Severely Neutropenic Mice That Survive and Breed in Homozygous Form. J Immunol 201, 3793–3803. [PubMed: 30464050]

Curnutte JT, Whitten DM, and Babior BM (1974). Defective superoxide production by granulocytes from patients with chronic granulomatous disease. N Engl J Med 290, 593–597. [PubMed: 4359964]

Dastgheyb SS, Villaruz AE, Le KY, Tan VY, Duong AC, Chatterjee SS, Cheung GY, Joo HS, Hickok NJ, and Otto M (2015). Role of Phenol-Soluble Modulins in Formation of Staphylococcus aureus Biofilms in Synovial Fluid. Infect Immun 83, 2966–2975. [PubMed: 25964472]

Dzhagalov I, St John A, and He YW (2007). The antiapoptotic protein Mcl-1 is essential for the survival of neutrophils but not macrophages. Blood 109, 1620–1626. [PubMed: 17062731]

Foster TJ, Geoghegan JA, Ganesh VK, and Hook M (2014). Adhesion, invasion and evasion: the many functions of the surface proteins of Staphylococcus aureus. Nat Rev Microbiol 12, 49–62. [PubMed: 24336184]

Geiger T, Francois P, Liebeke M, Fraunholz M, Goerke C, Krismer B, Schrenzel J, Lalk M, and Wolz C (2012). The stringent response of Staphylococcus aureus and its impact on survival after phagocytosis through the induction of intracellular PSMs expression. PLoS Pathog 8, e1003016. [PubMed: 23209405]

Gillaspy AF, Hickmon SG, Skinner RA, Thomas JR, Nelson CL, and Smeltzer MS (1995). Role of the accessory gene regulator (agr) in pathogenesis of staphylococcal osteomyelitis. Infect Immun 63, 3373–3380. [PubMed: 7642265]

Grosz M, Kolter J, Paprotka K, Winkler AC, Schafer D, Chatterjee SS, Geiger T, Wolz C, Ohlsen K, Otto M, et al. (2014). Cytoplasmic replication of Staphylococcus aureus upon phagosomal escape triggered by phenol-soluble modulin alpha. Cell Microbiol 16, 451–465. [PubMed: 24164701]

Guerra FE, Borgogna TR, Patel DM, Sward EW, and Voyich JM (2017). Epic Immune Battles of History: Neutrophils vs. Staphylococcus aureus. Front Cell Infect Microbiol 7, 286. [PubMed: 28713774]

Heyer G, Saba S, Adamo R, Rush W, Soong G, Cheung A, and Prince A (2002). Staphylococcus aureus agr and sarA functions are required for invasive infection but not inflammatory responses in the lung. Infect Immun 70, 127–133. [PubMed: 11748173]

Hill HR, Ochs HD, Quie PG, Clark RA, Pabst HF, Klebanoff SJ, and Wedgwood RJ (1974). Defect in neutrophil granulocyte chemotaxis in Job's syndrome of recurrent "cold" staphylococcal abscesses. Lancet 2, 617–619. [PubMed: 4137601]

Horn J, Stelzner K, Rudel T, and Fraunholz M (2018). Inside job: Staphylococcus aureus host-pathogen interactions. Int J Med Microbiol 308, 607–624. [PubMed: 29217333]

Howard MW, Strauss RG, and Johnston RB Jr. (1977). Infections in patients with neutropenia. Am J Dis Child 131, 788–790. [PubMed: 327794]

Introne W, Boissy RE, and Gahl WA (1999). Clinical, molecular, and cell biological aspects of Chediak-Higashi syndrome. Mol Genet Metab 68, 283–303. [PubMed: 10527680]

Kobayashi SD, Malachowa N, Whitney AR, Braughton KR, Gardner DJ, Long D, Bubeck Wardenburg J, Schneewind O, Otto M, and Deleo FR (2011). Comparative analysis of USA300 virulence determinants in a rabbit model of skin and soft tissue infection. J Infect Dis 204, 937–941. [PubMed: 21849291]

Ley K, Hoffman HM, Kubes P, Cassatella MA, Zychlinsky A, Hedrick CC, and Catz SD (2018). Neutrophils: New insights and open questions. Sci Immunol 3.

Li M, Dai Y, Zhu Y, Fu CL, Tan VY, Wang Y, Wang X, Hong X, Liu Q, Li T, et al. (2016). Virulence determinants associated with the Asian community-associated methicillin-resistant Staphylococcus aureus lineage ST59. Sci Rep 6, 27899. [PubMed: 27296890]

Liu H, Archer NK, Dillen CA, Wang Y, Ashbaugh AG, Ortines RV, Kao T, Lee SK, Cai SS, Miller RJ, et al. (2017). Staphylococcus aureus Epicutaneous Exposure Drives Skin Inflammation via IL-36-Mediated T Cell Responses. Cell Host Microbe 22, 653–666 e655. [PubMed: 29120743]

Lowy FD (1998). Staphylococcus aureus infections. N Engl J Med 339, 520–532. [PubMed: 9709046]

Munzenmayer L, Geiger T, Daiber E, Schulte B, Autenrieth SE, Fraunholz M, and Wolz C (2016). Influence of Sae-regulated and Agr-regulated factors on the escape of Staphylococcus aureus from human macrophages. Cell Microbiol 18, 1172–1183. [PubMed: 26895738]

Nakagawa S, Matsumoto M, Katayama Y, Oguma R, Wakabayashi S, Nygaard T, Saijo S, Inohara N, Otto M, Matsue H, et al. (2017). Staphylococcus aureus Virulent PSMalpha Peptides Induce Keratinocyte Alarmin Release to Orchestrate IL-17-Dependent Skin Inflammation. Cell Host Microbe 22, 667–677 e665. [PubMed: 29120744]

Nakamura Y, Oscherwitz J, Cease KB, Chan SM, Munoz-Planillo R, Hasegawa M, Villaruz AE, Cheung GY, McGavin MJ, Travers JB, et al. (2013). Staphylococcus delta-toxin induces allergic skin disease by activating mast cells. Nature 503, 397–401. [PubMed: 24172897]

Nakamura Y, Takahashi H, Takaya A, Inoue Y, Katayama Y, Kusuya Y, Shoji T, Takada S, Nakagawa S, Oguma R, et al. (2020). Staphylococcus Agr virulence is critical for epidermal colonization and associates with atopic dermatitis development. Sci Transl Med 12.

Novick RP (2003). Autoinduction and signal transduction in the regulation of staphylococcal virulence. Mol Microbiol 48, 1429–1449. [PubMed: 12791129]

Nygaard TK, Pallister KB, Ruzevich P, Griffith S, Vuong C, and Voyich JM (2010). SaeR binds a consensus sequence within virulence gene promoters to advance USA300 pathogenesis. J Infect Dis 201, 241–254. [PubMed: 20001858]

Pang YY, Schwartz J, Thoendel M, Ackermann LW, Horswill AR, and Nauseef WM (2010). agr-Dependent interactions of Staphylococcus aureus USA300 with human polymorphonuclear neutrophils. J Innate Immun 2, 546–559. [PubMed: 20829608]

Peschel A, and Otto M (2013). Phenol-soluble modulins and staphylococcal infection. Nat Rev Microbiol 11, 667–673. [PubMed: 24018382]

Queck SY, Jameson-Lee M, Villaruz AE, Bach TH, Khan BA, Sturdevant DE, Ricklefs SM, Li M, and Otto M (2008). RNAIII-independent target gene control by the agr quorum-sensing system: insight into the evolution of virulence regulation in Staphylococcus aureus. Mol Cell 32, 150–158. [PubMed: 18851841]

Soehnlein O, and Lindbom L (2010). Phagocyte partnership during the onset and resolution of inflammation. Nat Rev Immunol 10, 427–439. [PubMed: 20498669]

Surewaard BG, de Haas CJ, Vervoort F, Rigby KM, DeLeo FR, Otto M, van Strijp JA, and Nijland R (2013). Staphylococcal alpha-phenol soluble modulins contribute to neutrophil lysis after phagocytosis. Cell Microbiol 15, 1427–1437. [PubMed: 23470014]

Surewaard BG, Nijland R, Spaan AN, Kruijtzer JA, de Haas CJ, and van Strijp JA (2012). Inactivation of staphylococcal phenol soluble modulins by serum lipoprotein particles. PLoS Pathog 8, e1002606. [PubMed: 22457627]

Wang R, Braughton KR, Kretschmer D, Bach TH, Queck SY, Li M, Kennedy AD, Dorward DW, Klebanoff SJ, Peschel A, et al. (2007). Identification of novel cytolytic peptides as key virulence determinants for community-associated MRSA. Nat Med 13, 1510–1514. [PubMed: 17994102]

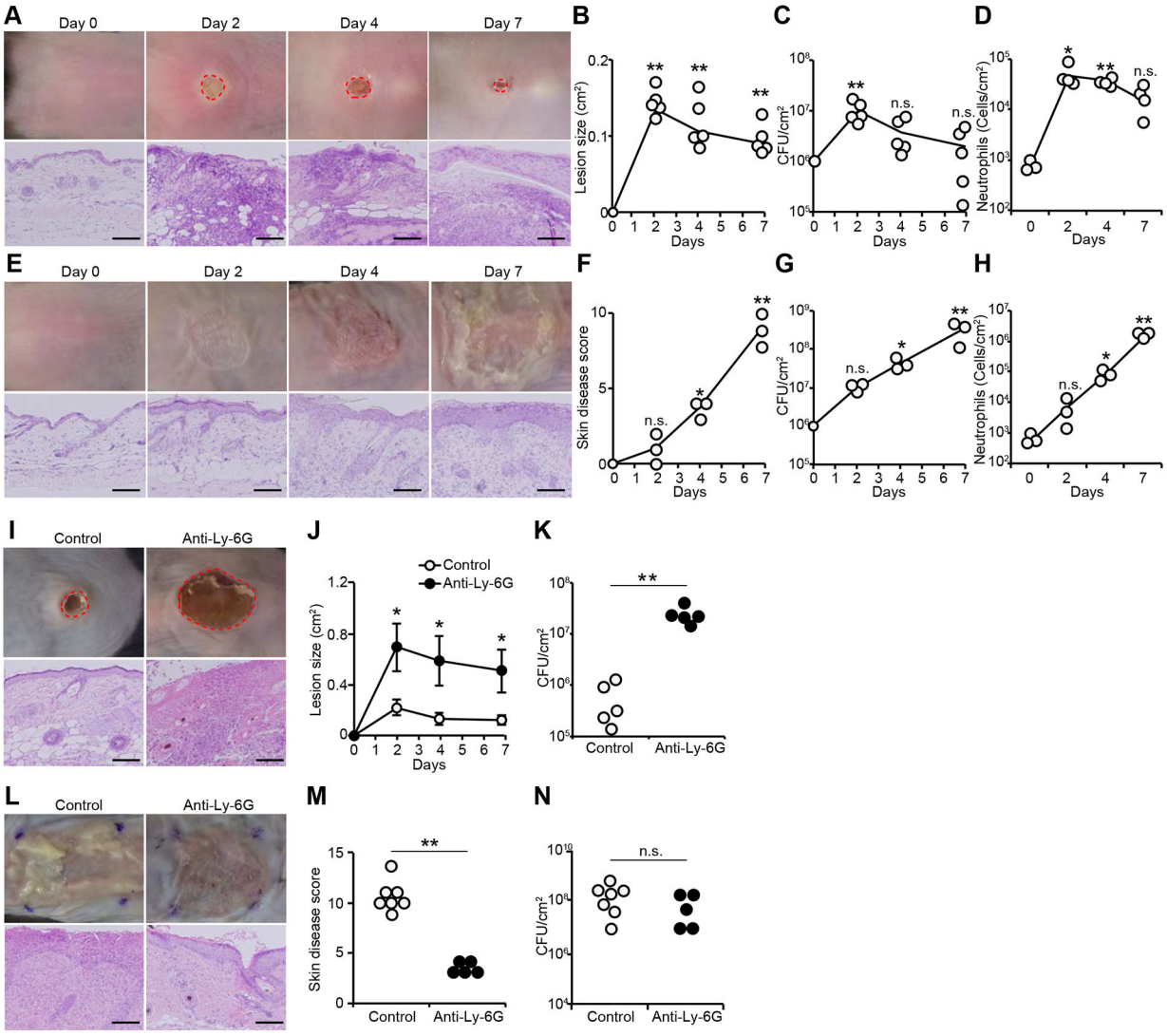


**Figure 1. Differential role of neutrophils in epidermal and intradermal *S. aureus* infection.**

**A-H**, C57BL/6 mice were intradermally (**A-D**) and epicutaneously (**E-H**) inoculated with *S. aureus.* Representative macroscopic images of mouse skin and hematoxylin and eosin (HE)-stained skin sections on day 7 after colonization (n=3 to 5 mice per group) (**A** and **E**). Skin lesion size (**B**), numbers of *S. aureus* colony forming unit (cfu) (**C** and **G**), numbers of neutrophils (**D** and **H**) and skin disease scores (**F**) in the skin of WT mice at indicated time point after infection. **I-N**, Mice treated with control Mab and anti-Ly6G Mab were intradermally (**I-K**) and epicutaneously (**L-N**) inoculated with *S. aureus.* Representative macroscopic images of mouse skin and HE-stained skin sections on day 7 after colonization (n=5 to 7 mice per group) (**I** and **L**). Skin lesion size at indicated time point (**J**). Number of *S. aureus* cfu (**K** and **N**) and skin disease score (**M**) in the skin of mice 7 days after infection. Data are presented as mean ± SEM (**B, C, D, F, G, H, J** and **K**). Each dot represents a mouse (**B, C, D, F, G, H, K, M** and **N**). Skin lesions are highlighted by dotted red circles (**A** and **I**). Data are representative of at least two independent experiments. Scale bars, 100 μm. n.s.; not significant, *P<0.05; **P<0.01 versus control Mab or day 0, by unpaired two-tailed

Mann-Whitney U test (**K, M** and **N**), two-tailed Student's t test (**J**), one-way ANOVA test with Bonferroni's correction (**F** and **G**) or Kruskal-Wallis test (**B, C, D** and **H**). See also Figure S1.

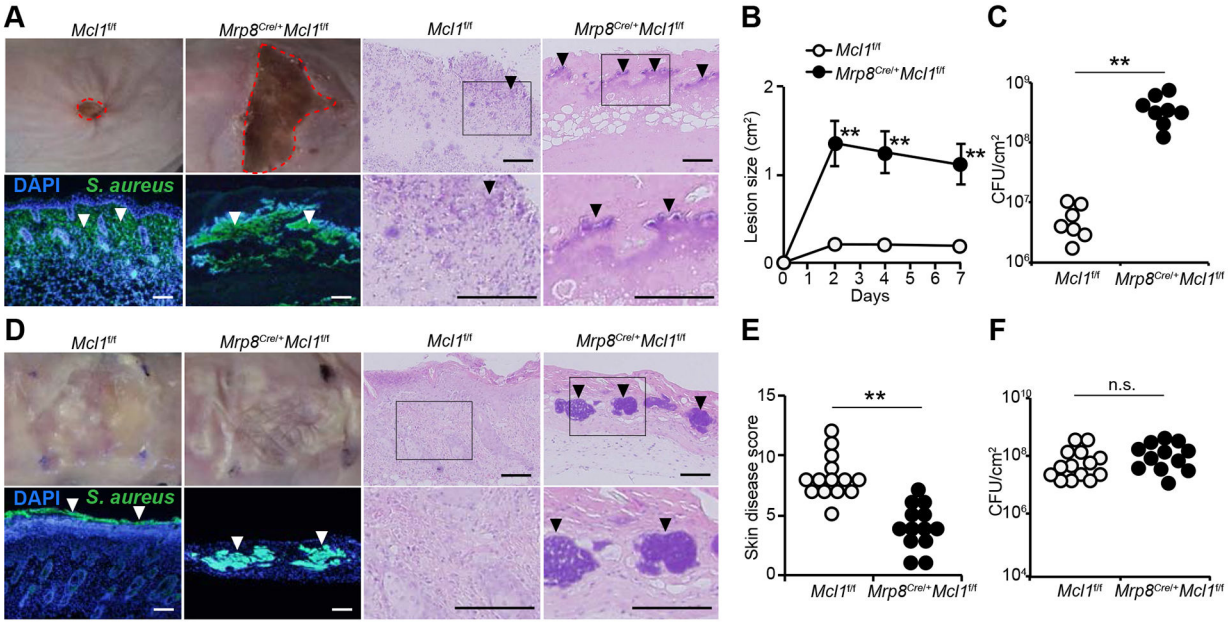


**Figure 2. Neutrophils are required to prevent *S. aureus* invasion into the dermis.**

**A-F**, *Mcl1*$^{f/f}$ and *Mrp8*$^{Cre/+}$*Mcl1*$^{f/f}$ mice were intradermally (**A-C**) and epicutaneously (**D-F**) inoculated with *S. aureus.* Representative macroscopic images of mouse skin, immunohistochemical sections and HE-stained skin sections on day 7 after infection (n=7 to 8 mice per group (**A**) and n=13 to 14 mice per group (**D**)). Skin lesion size at indicated time point (**B**). The number of *S. aureus* cfu (**C** and **F**) and skin disease scores (**E**) in the skin of *Mcl1*$^{f/f}$ and *Mrp8*$^{Cre/+}$*Mcl1*$^{f/f}$ mice 7 days after infection. Data are presented as mean ± SEM (**B** and **C**). Each dot represents a mouse (**C, E** and **F**). Skin lesions are highlighted by dotted red circles. Black arrowheads show bacteria in HE sections (purple areas), white arrowheads show immune-labeled bacteria. Data represent combined results from at least two independent experiments. Scale bars, 100 μm. n.s.; not significant, *P<0.05; **P<0.01 versus *Mcl1*$^{f/f}$ mice, by unpaired two-tailed Mann-Whitney U test (**B, E** and **F**) or two-tailed Student's t test (**C**). See also Figure S2.

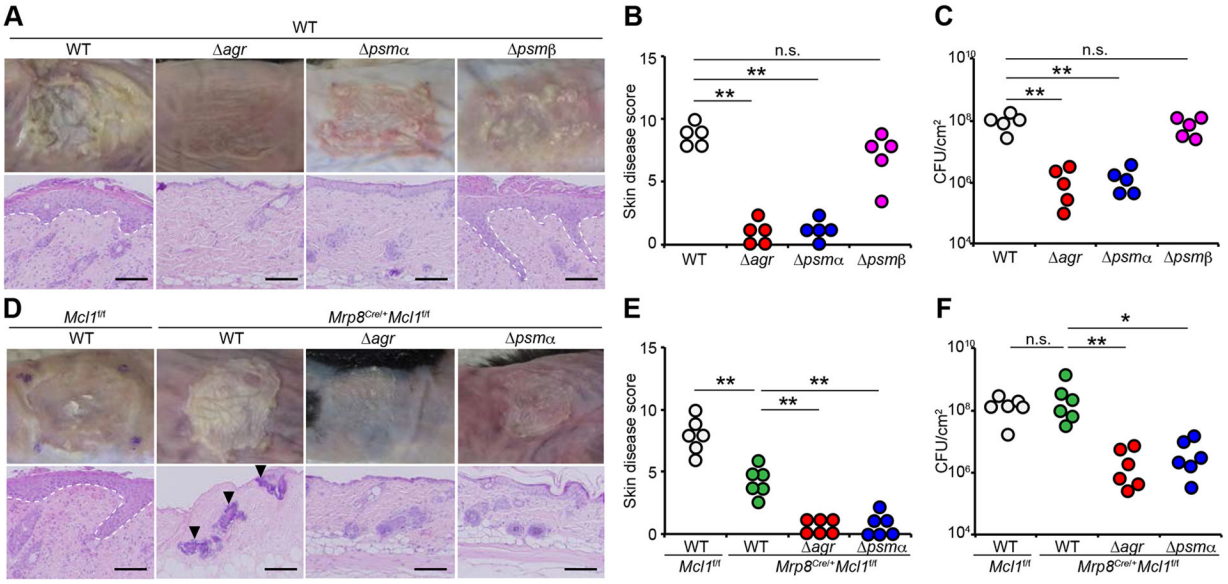


**Figure 3. Agr-regulated PSMα peptides are required for pathogen dermal invasion in the absence of neutrophils.**

**A-F**, *Mcl1*$^{f/f}$ and *Mrp8*$^{Cre/+}$*Mcl1*$^{f/f}$ mice were epicutaneously inoculated with WT or the indicated isogenic mutant *S. aureus* strains. Representative macroscopic images of mouse skin and HE-stained skin sections on day 7 after infection (n=5 to 6 mice per group) (**A** and **D**). Skin disease scores (**B** and **E**) and the number of *S. aureus* cfu (**C** and **F**) in the skin of *Mcl1*$^{f/f}$ and *Mrp8*$^{Cre/+}$*Mcl1*$^{f/f}$ mice 7 days after infection. Each dot represents a mouse (**B, C, E** and **F**). Arrowheads show bacteria. Thickened epidermis is outlined by dotted line. Data are representative of at least two independent experiments. n.s.; not significant, *P<0.05; **P<0.01, by Kruskal-Wallis test (**B, C, E** and **F**).

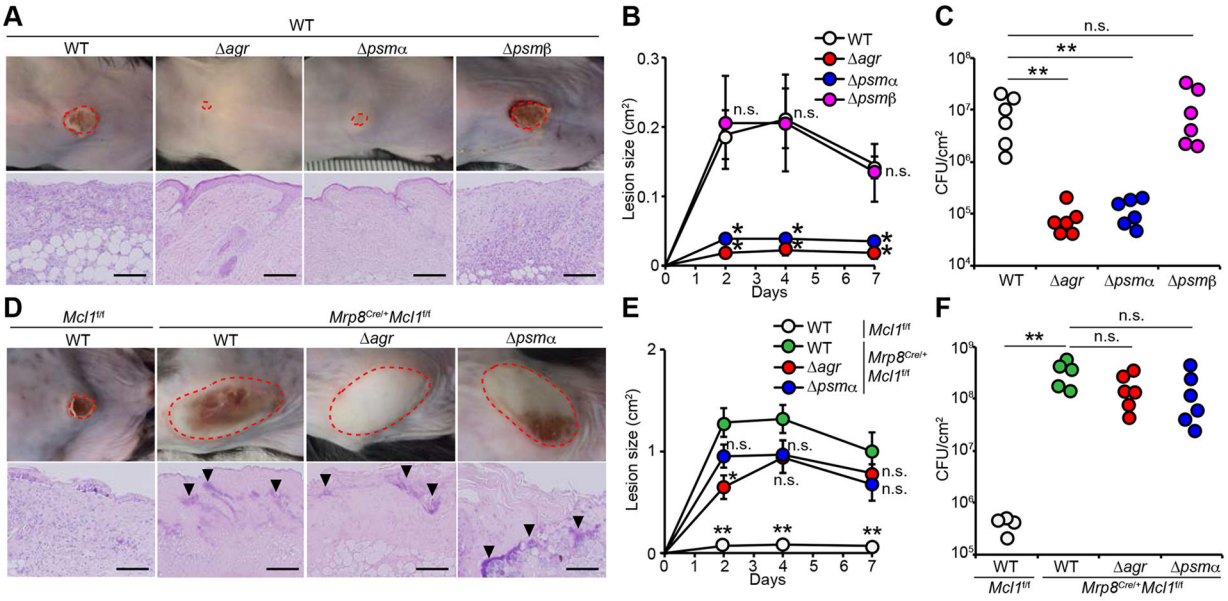


**Figure 4. PSMα peptides are not required for intradermal *S. aureus* growth in the absence of neutrophils.**

**A-F**, WT, *Mcl1*$^{f/f}$ and *Mrp8*$^{Cre/+}$*Mcl1*$^{f/f}$ mice were intradermally inoculated with WT or the indicated isogenic mutant *S. aureus* strains. Representative macroscopic images and HE-stained skin sections on day 7 after infection (n=4 to 6 mice per group) (**A** and **D**). Skin lesion size at indicated time point (**B** and **E**). The number of *S. aureus* cfu in the skin of mice 7 days after infection (**C** and **F**). Data are presented as mean ± SEM (**B, C, E** and **F**). Skin lesions are highlighted by dotted red circles. Arrowheads show bacteria. Data represent combined results from at least two independent experiments. Scale bars, **100** μm. n.s.; not significant, *P<0.05; **P<0.01 versus, by Kruskal-Wallis test (**B, C, E** and **F**). See also Figure S3.

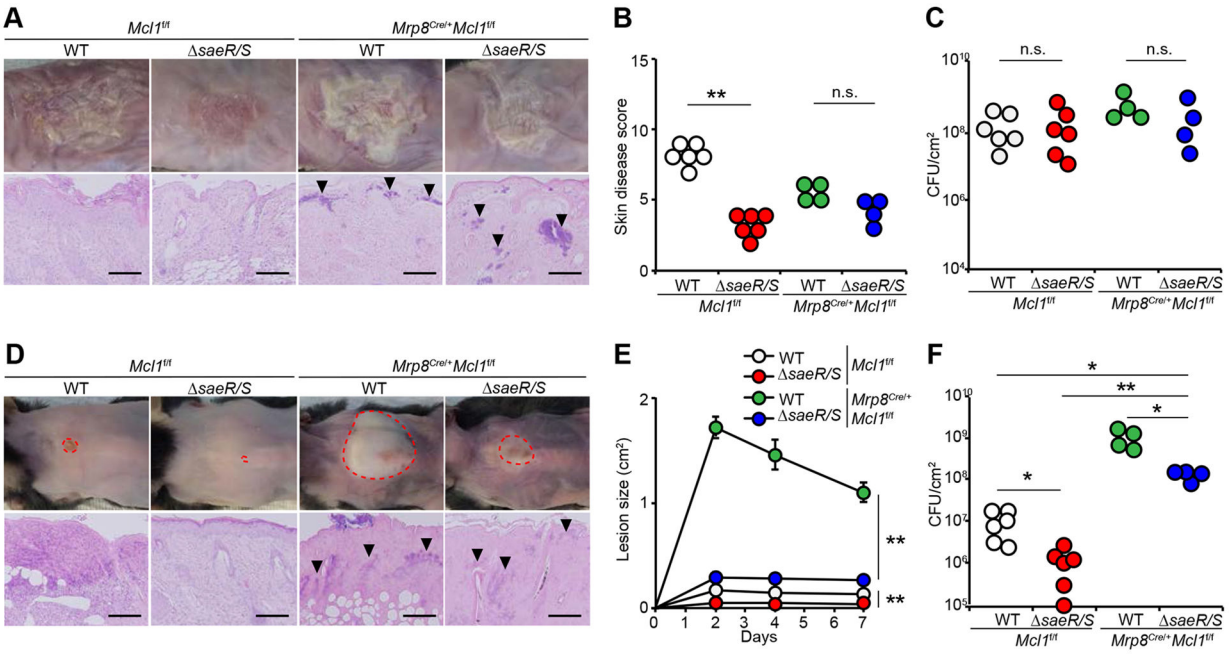


**Figure 5. SaeR/S virulence is critical for intradermal *S. aureus* growth in the absence of neutrophils.**

**A-F**, *Mcl1*$^{f/f}$ and *Mrp8*$^{Cre/+}$*Mcl1*$^{f/f}$ mice were epicutaneously (**A-C**) and intradermally (**D-F**) inoculated with WT or the isogenic *saeR/S* mutant *S. aureus* strain. Representative macroscopic images and HE-stained skin sections on day 7 after infection (n=4 to 6 mice per group) (**A** and **D**). Skin disease scores (**B**) and the number of *S. aureus* cfu (**C** and **F**) in the skin of *Mcl1*$^{f/f}$ and *Mrp8*$^{Cre/+}$*Mcl1*$^{f/f}$ mice 7 days after infection. Skin lesion size at indicated time point (**E**). Each dot represents a mouse (**B, C** and **F**). Data are presented as mean ± SEM (**E** and **F**). Skin lesions are highlighted by dotted red circles (**D**). Black arrowheads show bacteria. Data represent combined results from at least two independent experiments. Scale bars, 100 μm. n.s.; not significant, *P<0.05; **P<0.01, by Kruskal-Wallis test (**B, C, E** and **F**). See also Figure S4.

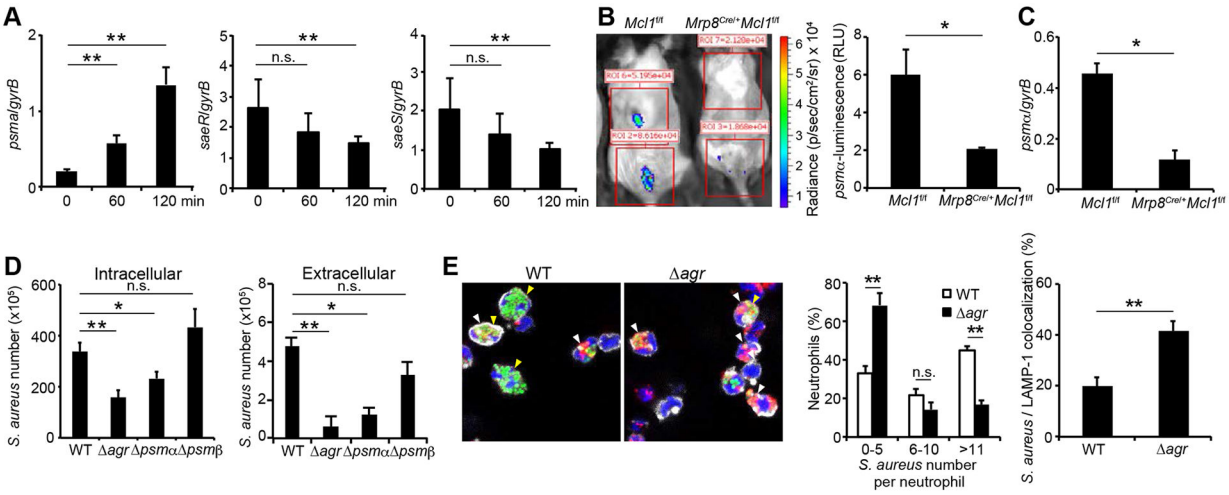


**Figure 6. Agr virulence limits the localization of *S. aureus* in late endosomes and promotes phagosome escape into the cytosol.**

**A,** *psmα*, *saeR* and *saeS* expression levels in neutrophils after incubation with WT *S. aureus* at a moi of 5 for 15 min, removal of extracellular bacteria (time 0 min) and further incubation for indicated times. **B**, $Mcl1^{f/f}$ and $Mrp8^{Cre/+}Mcl1^{f/f}$ mice were intradermally inoculated with *psm*α-lux *S. aureus* for 2 days. Luminescence of *psmα-lux* (relative light units) is indicated on the right panel. (n=4 mice per group). **C,** *psmα* expression in the skin of $Mcl1^{f/f}$ and $Mrp8^{Cre/+}Mcl1^{f/f}$ mice intradermally inoculated with WT *S. aureus*. **D**, The numbers of *S. aureus* in intracellular and extracellular compartments of WT neutrophils cultured with WT and the indicated mutant *S. aureus* strains (moi =5) for 15 min, washed and then incubated in the presence of recombinant TNF-α for 1 hour to induce oxidative burst (total 80 min). **E**, Representative microscopic images of WT neutrophils cultured with YFP-WT and YFP-*agr* mutant *S. aureus* (moi=5) for 15 min and then incubated in the presence of recombinant TNF-α for 1 h (total 80 min). Neutrophils with YFP-*S. aureus* (green) were stained with DAPI (blue) and fluorescence-labeled antibodies against Ly6G (white) and LAMP-1 (red). The percentage of neutrophils containing different numbers of WT (white bars) and *agr* mutant (black bars) YFP-*S. aureus* and the percentage of neutrophils in which bacteria co-localized with LAMP-1 inside neutrophils are indicated on the right panel. White arrowheads show neutrophils in which intracellular bacteria co-localize with LAMP-1. Yellow arrowheads show neutrophils with high (greater than 10) intracellular bacteria. Neutrophils cultured with YFP-WT (n=233) and YFP-agr *S. aureus* (n=193) were enumerated from 8 fields per group. Data are presented as mean ± SEM. Data are representative of at least two independent experiments. n.s.; not significant, *P<0.05; **P<0.01, by one-way ANOVA test with Bonferroni's correction (**A**), unpaired two-tailed Mann-Whitney U test (**B, C** and **E**) or Kruskal-Wallis test (**D**). See also Figure S5.

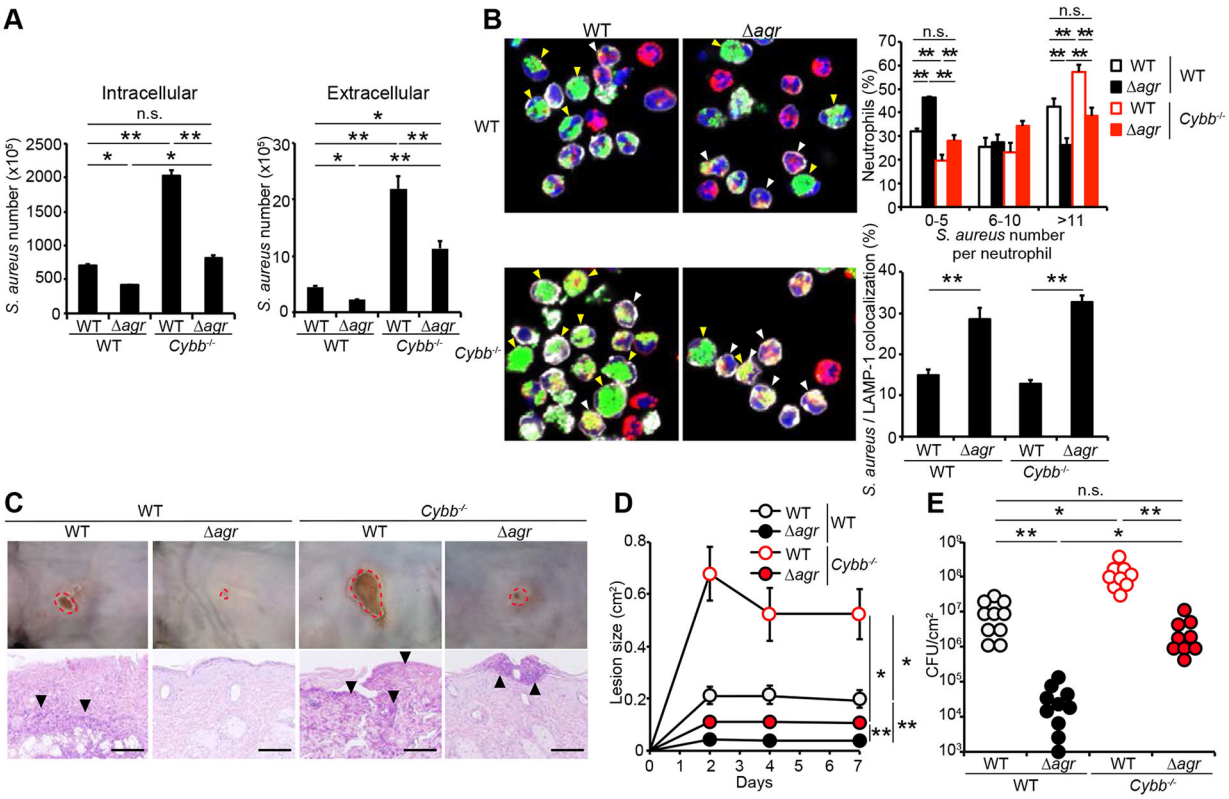


**Figure 7. Agr virulence limits oxidative and non-oxidative pathogen killing in vivo.**

**A**, Numbers of *S. aureus* in intracellular and extracellular compartments of WT and *Cybb*$^{-/-}$ neutrophils cultured with WT and *agr* mutant *S. aureus* strains (moi =5) for 15 min and then incubated in the presence of recombinant TNF-α for 1 hour (total 80 min). **B**, Representative microscopic images of WT and *Cybb*−/− neutrophils cultured with YFP-WT and YFP-*agr* mutant *S. aureus* (moi =5) for 15 min, washed and further incubated in the presence of recombinant TNF-α for 1 h (total 80 min). Neutrophils with YFP-*S. aureus* (green) were stained with DAPI (blue) and fluorescence-labeled antibodies against Ly6G (white) and LAMP-1 (red). The percentage of neutrophils containing different numbers of WT (open bars) and *agr* mutant (solid bars) YFP-*S. aureus* and the percentage of neutrophils in which bacteria co-localized with LAMP-1 inside neutrophils are indicated on right panels. White arrowheads show neutrophils in which intracellular bacteria co-localized with LAMP-1. Yellow arrowheads show neutrophils with high (greater than 10) intracellular bacteria. The percentage of bacteria in WT neutrophils cultured with YFP-WT (n=156) and YFP-agr mutant *S. aureus* (n=172) and *Cybb*$^{-/-}$ neutrophils cultured with YFP-WT (n=127) and YFP-agr mutant *S. aureus* (n=166) were enumerated from 8 different fields per group. **C-E**, WT and *Cybb*$^{-/-}$ mice were intradermally inoculated with WT and *agr* mutant *S. aureus* strains. Representative macroscopic images of mouse skin and HE-stained skin sections on day 7 after colonization (n=9 to 10 mice per group) (**C**). Skin lesion size at indicated time point (**D**). The number of *S. aureus* cfu in the skin of WT and *Cybb*$^{-/-}$ mice 7 days after infection (**E**). Data are presented as mean ± SEM (**A, B, D** and **E**). Skin lesions are highlighted by dotted red circles and arrowheads show bacteria (**C**). Data

are representative of at least two independent experiments. n.s.; not significant, *P<0.05; **P<0.01, by Kruskal-Wallis test (**A, B, D** and **E**). See also Figure S6.

## KEY RESOURCES TABLE

| REAGENT or RESOURCE | SOURCE | IDENTIFIER |
|---|---|---|
| Antibodies | | |
| Alexa Fluor 555 goat polyclonal anti-rabbit IgG | Abcam | Cat# ab150078 |
| APC anti-Ly6G | BioLegend | Cat# 127614; RRID: AB_2227348 |
| APC anti-Ly6C | BD Biosciences | Cat# 560595; RRID: AB_1727554 |
| Biotin rabbit polyclonal anti-*S. aureus* | Abcam | Cat# ab68954; |
| FITC anti-CD11b | BioLegend | Cat# 101205; RRID: AB_312788 |
| PE anti-CD107a (LAMP-1) | BioLegend | Cat# 121611; RRID: AB_1732051 |
| PE anti-B220 | BioLegend | Cat# 103208; RRID: AB_312993 |
| PE anti-F4/80 | eBioscience | Cat# 12-4801-80; RRID: AB_465923 |
| PE anti-Gr1 | BD Biosciences | Cat# 553128; RRID: AB_394644 |
| PE anti-Ly6G | BioLegend | Cat# 127608; RRID: AB_1186099 |
| PECy7 anti-CD8 | eBioscience | Cat# 25-0081-81; RRID: AB_469583 |
| PerCP5.5 anti-CD4 | BioLegend | Cat# 100540; RRID: AB_893326 |
| Rabbit monoclonal anti-Rab5 (clone EPR21801) | Abcam | Cat# ab218624 |
| Rat monoclonal anti-mouse CD16/32 (clone 93) | BioLegend | Cat# 101302; RRID: AB_312801 |
| Rat monoclonal anti-mouse Ly6G (clone 1A8) | BioXCell | Cat# BE0075-1 |
| Rat monoclonal IgG2a isotype control (clone 2A3) | BioXCell | Cat# BE0089 |
| Violet 450 anti-Ly6G | BD Biosciences | Cat# 560603; RRID: AB_1727564 |
| Bacterial and Virus Strains | | |
| *Staphylococcus aureus* LAC (USA300) wild-type | Dr. Michael Otto (Wang et al., 2007) | N/A |
| *Staphylococcus aureus* LAC (USA300) Δ*agr* | Dr. Michael Otto (Wang et al., 2007) | N/A |
| *Staphylococcus aureus* LAC (USA300) Δ*psmα* | Dr. Michael Otto (Wang et al., 2007) | N/A |
| *Staphylococcus aureus* LAC (USA300) Δ*psmβ* | Dr. Michael Otto (Wang et al., 2007) | N/A |
| *Staphylococcus aureus* LAC (USA300) *psmα-lux* | Dr. Michael Otto (Dastgheyb et al., 2015) | N/A |
| *Staphylococcus aureus* JE2 (USA300) YFP-wild-type | Dr. Christian Wolz (Münzenmayer et al., 2016) | N/A |
| *Staphylococcus aureus* JE2 (USA300) YFP-Δ*agr* | Dr. Christian Wolz (Münzenmayer et al., 2016) | N/A |
| *Staphylococcus aureus* LAC (USA300) wild-type | Dr. Jovanka M. Voyich (Nygaard et al., 2010) | N/A |
| *Staphylococcus aureus* LAC (USA300) Δ*saeR/S* | Dr. Jovanka M. Voyich (Nygaard et al., 2010) | N/A |
| Chemicals, Peptides, and Recombinant Proteins | | |
| DAPI | BioLegend | Cat# 422801 |

| REAGENT or RESOURCE | SOURCE | IDENTIFIER |
|---|---|---|
| DNase I | Sigma-Aldrich | Cat# DN25 |
| FITC-streptavidin | BioLegend | Cat# 405202 |
| Fixable Viability Dye eFluor 780 | eBioscience | Cat# 65-0865-14 |
| Fluorescent mounting medium | Dako | Cat# S3023 |
| Liberase DH | Roche | Cat# 447529 |
| Lysostaphin | Sigma-Aldrich | Cat# L7386 |
| Mannitol salt agar | Nissui | Cat# 05236 |
| Percoll | GE Healthcare | Cat# 17-0891-01 |
| Recombinant mouse TNF-α | BioLegend | Cat# 575204 |
| Vancomycin Hydrochloride | Fresenius Kabi | NDC 63323-314-61 |
| Critical Commercial Assays | | |
| E.Z.N.A. Bacterial RNA kit | Omega Bio-tek | Cat# R6950-01 |
| High Capacity RNA-to-cDNA Kit | Applied Biosystems | Cat# 4387406 |
| LDH Cytotoxicity Detection Kit | Takara Biochemicals | Cat# MK401 |
| Neutrophil Isolation Kit | Miltenyi Biotec | Cat# 130-097-658 |
| RPMI Medium 1640 | Gibco | Cat# 21870-076 |
| TaqMan™ Fast Advanced Master Mix | Applied Biosystems | Cat# 4444556 |
| Tegaderm™ Film | 3M | Cat# 1624W |
| TritonX-100 | Fisher Scientific | Cat# BP151-500 |
| Tryptic Soy Broth | BD Difco | Cat# 211825 |
| Experimental Models: Organisms/Strains | | |
| Mouse: C57BL/6J: WT | The Jackson Laboratory | JAX: 000664 |
| Mouse: *Cybb*$^{-/-}$: B6.129S-*Cybb*$^{tm1Din}$/J | The Jackson Laboratory | JAX: 002365 |
| Mouse: *Mrp8*$^{Cre/+}$ | Dr. Andres Hidalgo | MGI:4415239 |
| Mouse: *Mcl1*$^{f/f}$ | Dr. Andres Hidalgo | MGI:2684151 |
| Oligonucleotides | | |
| gyrB: forward 5’-CAAATGATCACAGCATTTGGTACAG-3’ | (Nygaard et al., 2010) | N/A |
| gyrB: reverse 5’-CGGCATCAGTCATAATGACGAT-3’ | (Nygaard et al., 2010) | N/A |
| gyrB: probe 5’-[FAM]-AATCGGTGGCGACTTTGATCTAGCGAAAG-[BHQ]-3’ | (Nygaard et al., 2010) | N/A |
| psmα: forward 5’-TATCAAAAGCTTAATCGAACAATTC-3’ | (Dastgheyb et al., 2015) | N/A |
| psmα: reverse 5’-CCCCTTCAAATAAGATGTTCATATC-3’ | (Dastgheyb et al., 2015) | N/A |
| psmα: probe 5’-[FAM]-AAAGACCTCCTTTGTTTGTTATGAAATCTTATTTACCAG-[BHQ]-3’ | (Dastgheyb et al., 2015) | N/A |
| saeS: forward 5’-CGTACATTCAGAGTAGAAAACTCTCGTAATAC-3’ | (Nygaard et al., 2010) | N/A |

| REAGENT or RESOURCE | SOURCE | IDENTIFIER |
|---|---|---|
| saeS: reverse 5'-GTTGCGCGAGTTCATTAGCTATATAT-3' | (Nygaard et al., 2010) | N/A |
| saeS: probe 5'-[FAM]-AGCCTAATCCAGAACCACCCGTT-[BHQ]-3' | (Nygaard et al., 2010) | N/A |
| saeR: forward 5'-CTGCCAAAACACAAGAACATGATAC-3' | (Nygaard et al., 2010) | N/A |
| saeR: reverse 5'-CTTGGACTAAATGGTTTTTTGACATAGT-3' | (Nygaard et al., 2010) | N/A |
| saeR: probe 5'-[FAM]-ATTTACGCCTTAACTTTAGGTGCAGAT-[BHQ]-3' | (Nygaard et al., 2010) | N/A |
| Software and Algorithms | | |
| NIS-Elements-confocal software | NIKON | https://www.microscope.healthcare.nikon.com/products/software/nis-elements/nis-elements-confocal |
| Living image Software | PerkinElmer | https://www.perkinelmer.com/lab-products-and-services/resources/in-vivo-imaging-software-downloads.html#LivingImage |
| FlowJo | FlowJo LLC | https://www.flowjo.com |
| Gen5™ | BioTek | https://www.biotek.com/products/software-robotics-software/gen5-microplate-reader-and-imager-software/ |
| Prism (GraphPad Software) | GraphPad | https://www.graphpad.com |